RF-Copybook: A Millimeter Level Calligraphy Copybook based on commodity RFID

LIQIONG CHANG, Northwest University, China
JIE XIONG, Singapore Management University, Singapore
JU WANG, Northwest University, China
XIAOJIANG CHEN*, Northwest University, China
YU WANG, University of North Carolina at Charlotte, USA
ZHANYONG TANG, Northwest University, China
DINGYI FANG, Northwest University, China

As one of the best ways to learn and appreciate the Chinese culture, Chinese calligraphy is widely practiced and learned all over the world. Traditional calligraphy learners spend a great amount of time imitating the image templates of reputed calligraphers. In this paper, we propose an RF-based Chinese calligraphy template, named *RF-Copybook*, to precisely monitor the writing process of the learner and provide detail instructions to improve the learner's imitating behavior. With two RFID tags attached on the brush pen and three antennas equipped at the commercial RFID reader side, RF-Copybook tracks the pen's 3-dimensional movements precisely. The key intuition behind RF-Copybook's idea is that: (i) when there is only direct path signal between the tag and the antenna, the phase measured at the reader changes linearly with the distance, (ii) the reader offers very fine-grained phase readings, thus a millimeter level accuracy of antenna-tag distance can be obtained, (iii) by combing multiple antenna-tag distances, we can quantify the writing process with stroke based feature models. Extensive experiments show that RF-Copybook is robust against the environmental noise and achieves high accuracies across different environments in the estimation of the brush pen's elevation angle, nib's moving speed and position.

CCS Concepts: • **Human-centered computing → Ubiquitous and mobile computing**;

Additional Key Words and Phrases: RFID, Phase, Antenna-tag Distance, Chinese Calligraphy

ACM Reference Format:
Liqiong Chang, Jie Xiong, Ju Wang, Xiaojiang Chen, Yu Wang, Zhanyong Tang, and Dingyi Fang. 2017. RF-Copybook: A Millimeter Level Calligraphy Copybook based on commodity RFID. *Proc. ACM Interact. Mob. Wearable Ubiquitous Technol.* 1, 4, Article 128 (December 2017), 19 pages. https://doi.org/10.1145/3161191

1 INTRODUCTION

Chinese calligraphy is the writing art of Chinese character and is one important genres of art in China [10, 11, 21, 31]. It can be enjoyed for its visual artistry and also contains the unique cultural elements of Chinese history.

*This is the corresponding author

This work is partially supported by the National Natural Science Foundation of China under Grant Nos. 61572402, 61672428, 61772422 and 61572347.

Authors' addresses: Liqiong Chang, Northwest University, China, changliqiong@stumail.nwu.edu.cn; Jie Xiong, Singapore Management University, Singapore, jxiong@smu.edu.sg; Ju Wang, Northwest University, China, wangju@nwu.edu.cn; Xiaojiang Chen, Northwest University, China, xjchen@nwu.edu.cn; Yu Wang, University of North Carolina at Charlotte, USA, yu.wang@uncc.edu; Zhanyong Tang, Northwest University, China, zytang@nwu.edu.cn; Dingyi Fang, Northwest University, China, dyf@nwu.edu.cn.

2474-9567/2017/12-ART128 $15.00
https://doi.org/10.1145/3161191

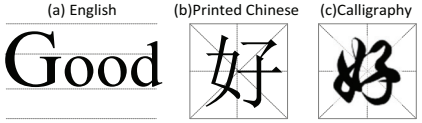

Fig. 1. A demo for the difference between English character, printed Chinese character and the Chinese calligraphy.

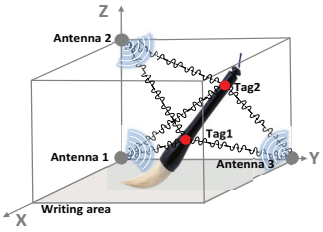

Fig. 2. A brief system setup: two tags are attached to the brush pen, three antennas are deployed to communicate with the tags.

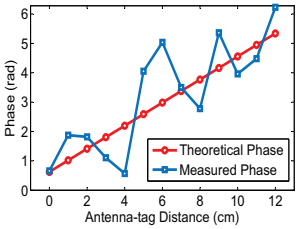

Fig. 3. Multipath effect breaks the linear relationship between antenna-tag distance and phase values.

Chinese calligraphy is widely practiced in China, Japan, Korea, and Vietnam. As one of the best ways to learn and appreciate the Chinese culture, we have seen a boom in calligraphy practising in the last few years due to the popularity of Chinese traditional cultures. More than 480 Confucius Institutes have been established all over the world by 2014 and this number will reach 1000 by 2020.

Most traditional calligraphy learners imitate strictly from image templates of reputed calligraphers [27, 33, 35]. Even a large amount of instructions are developed for the beginners, it still requires years of practice and usually experts' continuous feedback to improve the learner's skill. Several image based calligraphy feature analysis approaches are proposed in recent years to facilitate the learning [19, 30]. These approaches can track the difference between the leaner's writing and the template at a level of image pixel. However, in Chinese calligraphy, the stroke widths are variant and the relative location of each individual stroke with respect to the whole character is important, as shown in Fig. 1. Thus it is still challenging for the learner to conclude what changes need to be made to reduce the difference. The learner usually needs to empirically practice through many trials to slowly reduce the amount of difference.

In this paper, we designed an RF-based Chinese calligraphy template, RF-Copybook, which can precisely monitor the writing process of the learners at a millimeter level accuracy. In contrast to the traditional image templates, RF-Copybook provides detail instructions to guide the learner's imitating behavior. RF-Copybook is prototyped by attaching two cheap passive RFID tags on the brush pen and continuously collecting the phase and RSS readings at three antennas at the RFID reader side, as shown in Fig. 2. Then the writing process is customized into stroke-based models. The key intuition behind RF-Copybook's idea is that: if there is only direct path signal between the antenna and the tag on the brush pen, the phase changes linearly with the distance and thus we can estimate the distance information accurately. As commodity RFID reader is able to output very fine-grained phase readings, we can thus employ the phase readings to estimate the distance accurately. With two tags attached to the brush pen , RF-Copybook can track the brush pen's 3-dimensional movements precisely, thus providing detailed information of the writing process. There are multiple challenges before we can realize RF-Copybook as a practical system:

How to obtain 'clean' direct path phase values from the noisy readings? In the indoor environment, apart from the phase noise imposed by the hardware circuits, the multipath is another disruptive factor hindering the accurate distance estimation. The phase changes linearly with distance when there is only one path between the transmitter and receiver, shown in Fig. 3 as theoretical phase values. When multipath exists, the direct path signal and multipath signals are superimposed and the linear relationship between the phase readings and the distance is broken as shown in Fig. 3. Thus, we are not able to employ the phase readings for distance estimation any more. To retrieve the 'clean' direct path phase readings from the noisy measured data, we remove the random

hardware phase shifts through phase calibration. To eliminate the multipath effect, we find that if hopping among enough number of frequency channels, there will be channels with very little multipath. The channel with little multipath is identified when we observe a linear phase change with frequency. Note that different from Wi-Fi, RFID hops among 16 channels which are enough for us to select channels with very little multipath and we denote these channels as 'clean' channels. Based on this key observation, we can retrieve the 'clean' direct path phase readings for fine-grained distance estimation. We present the details in §3.

How to obtain accurate antenna-tag distance? Even after we obtain the 'clean' direct path phase readings, the antenna-tag distance still cannot be uniquely determined. The reason is that, when RF signal propagates in the air, the phase value rotates periodically. Every rotation of 2π corresponds to a propagation distance of one wavelength. Thus, multiple distance may exhibit a same phase change. To deal with this challenge, we observe that within a relatively small region, when the antenna-tag distance increases, the received signal strength (RSS) decreases dramatically. We thus employ the RSS measurement to determine the integer number of 2π phase rotations and then use the phase change to estimate the decimal part of the phase change. With one 'clean' channel, we obtain one distance estimation. Combining the distance estimation from multiple 'clean' channels can further improve the estimation accuracy. The details are shown in §4.

How to segment the phase readings into strokes? Before quantifying the writing process, we need to segment the phase readings into strokes. Every Chinese character is composed of a fixed number of strokes. The phase readings between two adjacent strokes are meaningless and need to be discarded. Traditional pause interval detection methods do not work well here because the writing pause between strokes are usually very small, especially for those accomplished calligraphers. Fortunately, we notice that during the process of ending one stroke to starting another stroke, the brush pen experiences a process of lifting up from the writing area, moving and then falling down to the writing area again. With this observation, we compute the nib's fine-grained elevation distance and accordingly segment each stroke as described in §5.

Based on the estimated antenna-tag distance, we need to quantify each character's writing features. Unlike the pencil or pen, the Chinese brush pen's flexible nib is very soft and the length change can be up to several centimetres. The nib is usually made of goat and wolf's hair and contributes to a myriad of writing possibilities. The unique feature of brush pen is reflected by the pen's movement with different *elevation angles* and *nib's length changes* which create variations in the width of strokes, and flexible *moving speeds* which generate smooth and aesthetical strokes. Another important feature of calligraphy is the relative *position* of each stroke in the whole character. We employ three antennas and use the fine-grained antenna-tag distances to model these factors for each stroke. Then the detailed differences for these factors between the calligrapher and the learner are extracted, providing instructions on improving the writing process of each stroke. The details are presented in §6. We summarize the contributions as follows:

- We design the first RF-based Chinese calligraphy monitoring system RF-Copybook to precisely depict the process of calligraphy writing.
- We propose a millimeter level antenna-tag distance estimation method by combining information from multiple 'clean' channels.
- We present and quantify four features to characterize the calligraphy writing process. The feature difference between the calligrapher and the learner is employed to guide the learner's practicing process.
- We implement RF-Copybook with commodity RFID device and evaluate the performance in different environments. The results demonstrate that in the low multipath hall environment, medium multipath office environment and high multipath library environment, RF-Copybook (i) achieves average antenna-tag distance estimation errors of 4.8 mm, 6.5 mm and 7.5 mm, respectively; (ii) segments the adjacent strokes at accuracies of 98%, 94% and 89%, respectively.

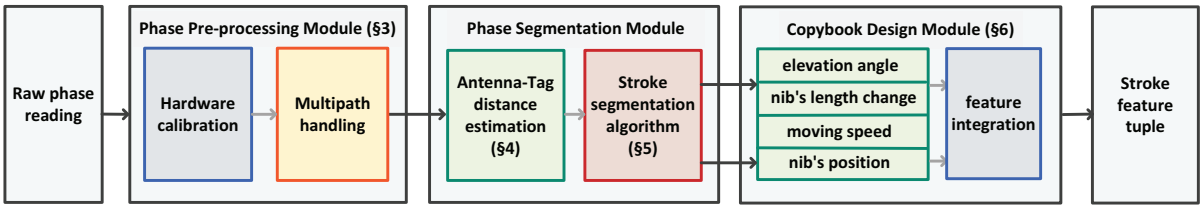

Fig. 4. System overview of RF-Copybook.

Note that we focus on the standard script type (kaishu) in RF-Copybook since it is the most popular one among five basic script types. We leave the other script types as the future work.

2 SYSTEM DESIGN

RF-Copybook is an RF based feature extraction system for the writing process of Chinese calligraphy. RF-Copybook employs one RFID reader equipped with three antennas and two tags are attached on the brush pen. RF-Copybook is composed of three modules as shown in Fig. 4:

- **The phase pre-processing module:** RF-Copybook collects the phase readings of the signals reflected from two tags and pre-processes them. Firstly, the hardware-induced errors, including the constant phase shift caused by the circuits and noise caused by random tag rotation are calibrated out. After that, the issue of multipath is addressed by identifying and employing only those 'clean' channels with little multipath for distance estimation.
- **The stroke segmentation module:** RF-Copybook segments the phase readings based on strokes. To do so, millimeter level antenna-tag distances are estimated and then the strokes are segmented based on the accurate tracking of the nib. When RF-Copybook detects the nib is off the paper, one stroke is considered to be finished.
- **The copybook design module:** RF-Copybook extracts four features to depict the detailed writing process. Multiple feature tuples for each stroke are obtained. Then the feature difference between the calligrapher and the learner is measured to guide the learner's writing process.

In the following sections, the details of each module are presented.

3 PHASE PRE-PROCESSING

In this section, we present the design of RF-Copybook's phase pre-processing module. The objective is to remove the hardware noise and address the multipath issue in indoor environment.

3.1 Hardware calibration

For an RFID system, the RFID reader emits the RF signal through the antennas, the tag receives the signal and backscatters the signal back to the RFID reader. Suppose the distance between the antenna and tag is d and the signal propagates along the direct path, the phase reading measured at the reader can be denoted as:

$$\phi_m = (\frac{2\pi}{\lambda} \times 2d + \delta) \ mod \ 2\pi, \tag{1}$$

$$\delta = \phi_s + \phi_n, \tag{2}$$

where λ is the signal wavelength, δ is the unwanted phase component caused by i) the hardware circuits which is a constant phase shift ϕ_s and ii) the random hardware phase noise ϕ_n. Besides the propagation in the air, the

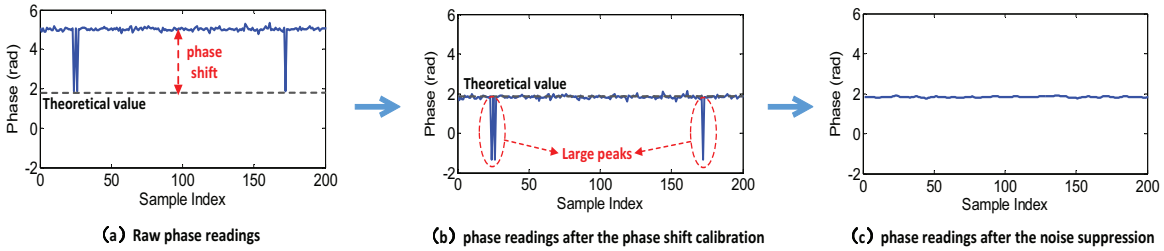

Fig. 5. Phase pre-processing.

hardware circuits and noise also cause phase rotations. Thus we need to remove δ from (1) before we can employ the phase to estimate the distance d.

Phase shift calibration. The constant phase shift ϕ_s above undermines the correct phase reading. To remove this phase offset, we place the tag very close to the antenna to reduce the amount of multipath and then measure the distance between the tag and antenna with a laser meter. With the measured ground truth distance, we can calculate the ground truth phase readings. The difference between the ground truth phase reading and the measured value is the phase shift ϕ_s we need to remove. Fig. 5 (a) and Fig. 5 (b) show the phase readings before and after the phase shift calibration. The distance between the antenna and the tag is set as $d = 37.1$ cm and the theoretical phase reading is [1] $\phi = 1.7988$.

Noise suppression. After removing the constant phase shift, we still observe some large peaks in phase readings due to random phase noise ϕ_n as shown in Fig. 5 (b). We first eliminate the abrupt phase changes by setting a threshold. If the phase difference between two continuous readings exceeds the threshold, we drop the later phase reading. Afterwards, we use the Kalman filter to smooth the phase readings. Fig. 5 (c) illustrates the phase values after the noise suppression process. It clearly shows that random peaks are removed.

3.2 Multipath handling

In real indoor environments, even the commodity RFID usually employs directional antennas and thus the multipath effect is not as severe as Wi-Fi, we can still observe the existence of multipath. If there is multipath, the received signal is a superposition of direct path signal and multi-path signals reflected from surrounding objects. Thus, the linear relationship between phase and distance we would employ for distance estimation does not hold any more. The pre-processing method introduced above removes the hardware-related phase offset and noises, it does not address the multipath issue.

We propose a multi-channel based method to identify those phase readings with little multipath. There are three reasons behind this method: (i) While commodity RFID readers employ directional antenna for transmissions, the amount of multipath is much less compared to Wi-Fi; (ii) As the tracking area of writing is relatively small, the distances between the RFID antennas and tags are also small. Thus the direct path signal is very strong and dominates, reducing the effect of multipath. (iii) Commodity RFID reader always hops among different channels during ordinary operations for security reasons. With a relatively large number (16) of channels available, we are able to identify quite a few channels affected by multipath very little (direct path dominates). At a given tag location, if there is no multipath, the phase difference $\Delta\phi$ measured at two channels with a central frequency

[1] The default central frequency for experiment is 924.375 MHz and the wavelength is 0.3245 m.

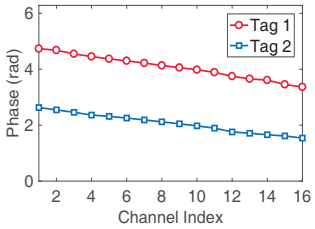

Fig. 6. Phase values at the hall environment.

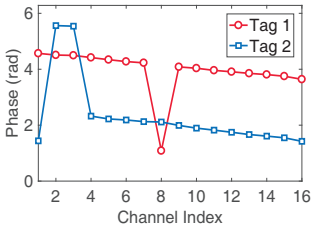

Fig. 7. Phase values at the office environment.

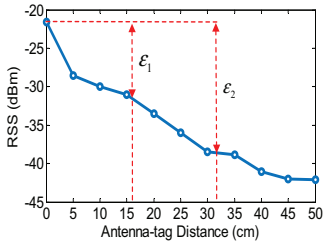

Fig. 8. RSS values with different antenna-tag distances.

difference of Δf can be denoted as:

$$\Delta\phi = (\frac{2\pi \times 2d}{c} \ mod \ 2\pi) \times \Delta f + \Delta\delta, \tag{3}$$

where c is the speed of light and $\Delta\delta$ is the phase noise. The phases at different channels exhibit a linear relationship. When multipath dominates, this linear relationship is broken. Fortunately, with a directional antenna and a small deployment area, the linear relationship still exists in the majority of channels and we term these channels *clean direct path channel*. That is to say, the signal at these clean channels propagates only through the direct path and the corresponding phase readings can be employed for distance estimation.

To validate this observation, we conduct benchmark experiments by hopping 16 different channels. The deployment scenarios are in a hall environment with low multipath level and an office environment with medium multipath level. Fig. 6 and Fig. 7 show the phase values at 16 different channels. In the hall scenario, we can observe very clear linear relationship. Even in the office scenario, we can still observe quite a few channels not affected by multipath and exhibit a linear relationship because of the small range deployment and directional antenna used in RFID systems.

4 ANTENNA-TAG DISTANCE ESTIMATION

In this section, we introduce the details about the antenna-tag distance estimation. After the phase processing, the relationship between antenna-tag distance d and phase value ϕ_m becomes:

$$\frac{2\pi \times f_m}{c} \times 2d = 2\pi \times k + \phi_m, \tag{4}$$

where k is an integer number indicating the number of 2π phase rotations. It is still challenging to estimate the distance d from (4) directly due to the unknown k.

To deal with this challenge, we employ the RSS measurement to estimate the value of k. Fig. 8 shows the RSS measurements with different antenna-tag distances at the clean direct path channel f_m. The RSS decreases when the distance between tag and antenna increases. That is to say, if the distance has a change of $\lambda/2$ with a corresponding phase rotation of 2π, although the phase reading is the same, the RSS change would be easily detected. Specifically, we set a proper RSS change threshold ε_k for each phase rotation number k. When the RSS difference exceeds the threshold, the corresponding phase rotation number k can be determined. In RF-Copybook, the value of k is 1 or 2. As the tracking area of writing is relatively small, the distances between the RFID antennas

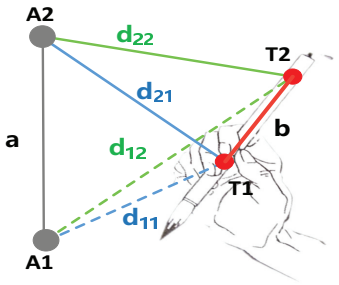

Fig. 9. Geometric restrictions among the antenna-tag distances.

and tags are also small[2]. Then, the antenna-tag distance can be obtained by:

$$d = \frac{c}{4\pi \times f_m} \times (2\pi \times k + \phi_m), \tag{5}$$

The phase reading resolution of the ImpinJ Speedway R420 RFID reader is 0.0015 radians [7]. This offers RF-Copybook possibility of estimating the antenna-tag distance to a millimeter level.

With the phase reading at one channel, RF-Copybook is able to obtain one distance estimate. We further employ the phase readings collected from multiple clean channels to improve the accuracy. Note that at different frequency channels, the phase rotation number remains unchanged. The ImpinJ R420 reader works at 16 channels with carrier frequencies ranged from 920.625 MHz to 924.375 MHz [7]. For two frequencies f_m and f_n to have a different phase rotation number k, the distance should be more than 40 m. The proof is presented in Section 10. In our deployment, the distance is smaller than 1 m and the RFID reader's operating range is about 10 m [7]. With different frequency channels, we obtain multiple solutions for the distance estimates. These results should be similar to each other and thus we can reject the outliers and also reject abnormal estimates based on geometric restrictions. As shown in Fig. 9, the distance between antenna 1 (A1) and antenna 2 (A2) is a, and the distance between tag 1 (T1) and tag 2 (T2) is b. Taking the triangle A2-T1-T2 as an example, the distances from antenna 2 to tag 1 d_{21} and to tag 2 d_{22} should satisfy the restriction that $d_{21} + d_{22} > b$ and $|d_{21} - d_{22}| < b$. There are a total of 4 groups of inequality equations restricting the estimated distances. After that, the estimates which simultaneously meet all the restrictions are selected for averaging to obtain the final distance estimate.

Finally, in order to obtain sufficient amount of data at locations when the brush pen is moving, we program the reader to hop only 8 channels rather than 16. The ImpinJ Speedway R420 reader is able to send about 150 frames per second [7]. We collect 8 packets at each location, one packet per channel, RF-Copybook is able to track 6 positions in 1 second with 3 antennas. After that, the distance sequence from antenna p to tag q when the pen moves with respect to timestamps can be denoted as $\mathbf{d}_{pq}$:

$$\mathbf{d}_{pq} = d_{pq}(t_1), d_{pq}(t_2), \cdots, d_{pq}(t_N), \tag{6}$$

where t_N is the timestamp, $p \in [1, 3]$ and $q \in [1, 2]$.

5 STROKE BASED PHASE SEQUENCE SEGMENTATION

During the writing process, even when the user is not writing a stroke, the brush pen is still moving and thus there are still phase changes. For example, when a user writes a Chinese character "Big" which is composed of

[2]Actually, if we keep tracking the phase changes, we know the transition point when phase value changes from 2π to a small value near to zero so the ambiguity of phase wrapping can be eliminated.

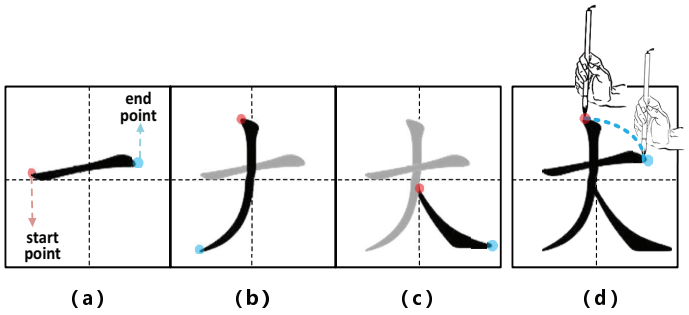

Fig. 10. (a), (b) and (c) are three strokes composing the Chinese character "Big"; (d) pen moves from the first stroke's end point to the second stroke's start point.

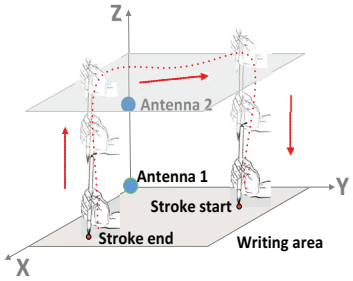

Fig. 11. Pen movement process during a meaningless stroke.

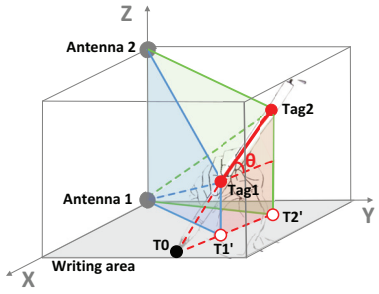

Fig. 12. The 3D location view of the brush pen and antennas.

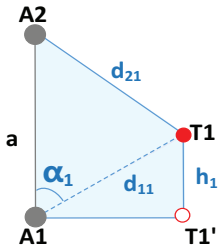

Fig. 13. Obtain the value of distance h_1.

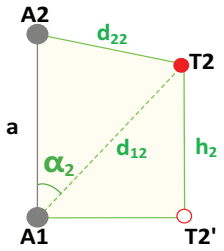

Fig. 14. Obtain the value of distance h_2.

three strokes (as shown in Fig. 10), there is no writing when the pen moves from the end point of the first stroke to the start point of the second stroke. However, the nib is moving and the phase is still changing. Thus, it is challenging to employ just phase readings to segment the strokes.

To cope with this challenge, we propose an elevation distance based segmentation method. The key observation is that — from the end of one stroke to start of the next stroke, the nib experiences a lifting from the writing area, moving in the air and then falling back to the writing area again, as shown in Fig. 11. Thus, the elevation height of the brush pen can be utilized to segment the strokes. We define the length from the pen's midpoint to the surface of the writing area as the pen's *elevation distance*. Fig. 12 shows a diagram when the brush pen is at one location of the writing area. We denote the distances from tag 1 and tag 2 to the writing area as h_1 and h_2 as shown in Fig. 13 and Fig. 14. We first compute the vertical distance h_1. The antenna-tag distances d_{21} and d_{11} can be computed by the method presented in §4. The antenna-antenna distance a and tag-tag distance b are known priori, hence h_1 can be computed as:

$$h_1 = d_{11} \times cos\alpha_1 = \frac{a^2 + d_{11}^2 - d_{21}^2}{2a}. \tag{7}$$

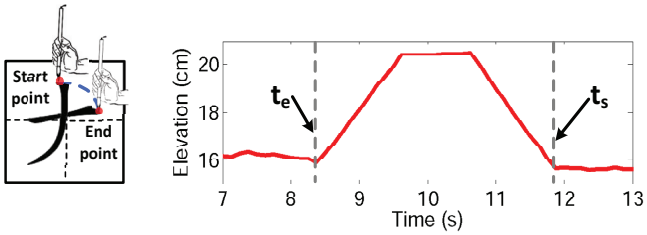

Fig. 15. The elevation distance changes during a meaningless stroke.

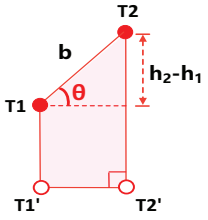

Fig. 16. Obtain the elevation angle θ.

In the same way, h_2 can be computed as:

$$h_2 = d_{12} \times cos\alpha_2 = \frac{a^2 + d_{12}^2 - d_{22}^2}{2a}. \tag{8}$$

Then the pen's elevation distance from the writing area can be expressed as:

$$h = \frac{h_1 + h_2}{2} = \frac{a}{2} + \frac{d_{11}^2 + d_{12}^2 - d_{11}^2 - d_{22}^2}{4a}. \tag{9}$$

We use the change of the pen's elevation distance h to segment the strokes. In principle, at the beginning and ending of each stroke, the brush pen is perpendicular. to the writing area. When the pen is lifted from the writing area, the value of h increases. And during the pen's translation movement between two strokes, the value of h keeps stable. Finally when the pen is elevated down to start the new stroke, h decreases. When the brush pen is writing a stoke, the h value may decrease significantly as the nib is soft and the length of the nib can change up to 2-3 cm. If the distance from the middle point of the two tags to the nib is h_p, we set a simple threshold $h_{t1} = h_p + \eta$ to detect the end of a stroke. Specifically, if h obtained in Equation 9 is larger than h_{t1}, we know the nib has left the writing area and one stroke is just finished. Once we detect h is smaller than $h_{t2} = h_p - \eta$, we conclude one new stroke is started. In our experiments, we set η as 5 mm. By doing so, the ending timestamp t_e and starting timestamp t_s can be obtained and used to segment a stroke as shown in Fig. 15.

6 CALLIGRAPHY COPYBOOK DESIGN

In this section, we first characterize the features which are important to Chinese calligraphy. Then we integrate these features to obtain each stroke's copybook.

Different from the rigid nibs of ordinary pens, the brush pen's soft nib is in a shape of an inverted cone made of animal's hair. When the hair absorbs ink and moves on the paper with different strengths and speeds, a significant amount of ink patterns are produced. Specifically, (i) the pen's different *elevation angles* and *nib's length changes* bring in variations in the stroke width; (ii) with different *moving speeds*, the stroke looks very different; (iii) the *nib's position and movement* determine each stroke's spatial location. If each stroke's relative position is not correct, even each individual stroke is perfect, the overall character will not look aesthetically. We interactively quantify these features.

6.1 Elevation angle

The elevation angle is the angle between the pen and the writing area. We denote the angle as θ and $\theta \in [0°, 90°]$. When the value of θ equals to 90°, the pen is perpendicular to the writing area. The bigger the elevation angle is, the smaller the stroke width is. θ is the angle formed by line T1T2 and T1'T2' shown in Fig. 16. Its value can thus

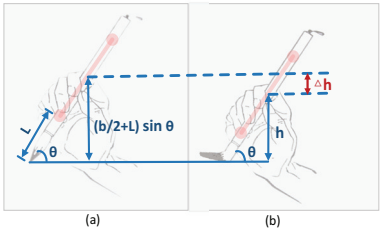

Fig. 17. The nib's length change Δh.

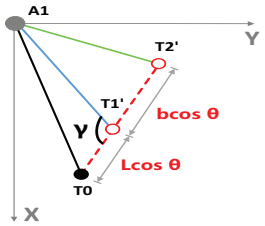

Fig. 18. Estimate the distance d_{10} from antenna1 A1 to the nib T0.

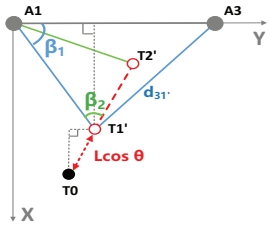

Fig. 19. Determine the nib position in the writing area $T0(x, y)$.

be computed as:

$$\theta = arcsin\ \frac{|h_2 - h_1|}{b} = arcsin\ \frac{d_{12}^2 + d_{21}^2 - d_{11}^2 - d_{22}^2}{2ab}. \tag{10}$$

6.2 Nib's length change

The nib's length change is another vital indicator reflecting the stroke's width. When the brush pen touches the writing area[3], different nib length changes can be created. Specifically, a large length change means the nib is touching a larger area, therefore the stroke has a wider width. As shown in Fig. 17, when the pen just touches the area with an elevation angle θ, the elevation distance is $(b/2 + L)sin\theta$ while L is the length from the tag 1 to the pen's nib. The elevation distance h can be obtained according to Eq.(9). Thus the downward displacement Δh is:

$$\Delta h = (b/2 + L)sin\theta - h. \tag{11}$$

6.3 Nib's Moving speed

The nib's moving speed is another key feature for Chinese calligraphy. The nib's moving speed can be calculated as the distance change rate between nib T0 and antenna 1 (A1). As shown in Fig. 18, the distance A1T0 can be denoted as $d_{10} = \sqrt{(Lcos\theta)^2 + d_{11'}^2 - 2Lcos\theta d_{11'}cos\gamma}$. Further, the value of $cos\gamma$ is $\frac{d_{11'}^2 + (bcos\theta)^2 - d_{12'}^2}{2d_{11'}bcos\theta}$ based on the Cosine law in triangle ΔA1T1'T2'. By plugging $cos\gamma$ into d_{10}, the distance A1T0 at time t_i thus is calculated as:

$$\begin{aligned} d_{10}(i) &= \sqrt{(Lcos\theta(i))^2 + d_{11'}^2(i) - 2Lcos\theta(i)d_{11'}(i) \times \frac{d_{11'}^2(i) + (bcos\theta(i))^2 - d_{12'}^2(i)}{2d_{11'}(i)bcos\theta(i)}}, \\ &= \sqrt{(1 + \frac{L}{b})d_{11'}^2(i) + (L^2 + bL)cos^2\theta(i) - \frac{L}{b}d_{12'}^2(i)}. \end{aligned} \tag{12}$$

And the nib's moving speed v is obtained by:

$$v(i) = \frac{\partial d_{10}}{\partial t} = \frac{d_{10}(i+1) - d_{10}(i)}{t_{i+1} - t_i}. \tag{13}$$

[3]We can use the pen's elevation distance together with the angle to determine whether the pen touches the writing area or not.

6.4 Nib's position

The nib's position $T0(x, y)$ on the writing area is a crucial indicator which reflects the stroke's spatial position within the whole character. As described in the above sections, we can accurately quantify the brush pen's elevation distance, elevation angle and moving speed with just two antennas. However, the pen's absolute position on the writing area is not fully constrained with only two antennas. Therefore, we add another antenna (antenna 3, referred as A3) at the Y-axis[4], as shown in Fig. 19. After we obtain the distance between A3 and T1' according to §4, the angle β_1 between line A1T1' and the Y-axis can be obtained. And now, the nib position $T0(x, y)$ can be determined by:

$$x = d_{11'} \sin\beta_1 + L\cos\theta \cdot \sin(\beta_2 + \beta_1), \tag{14}$$

$$y = d_{11'} \cos\beta_1 - L\cos\theta \cdot \cos(\beta_2 + \beta_1). \tag{15}$$

6.5 Integrate features into the stroke's copybook

The features above are quantified based on accurate antenna-tag distance estimation. At each timestamp, RF-Copybook calculates the antenna-tag distances and then obtains the pen's elevation angle, the nib's length change, nib's moving speed and nib's position subsequently. Now we integrate the features at different timestamps into a copybook for each stroke, hence the feature variations within a stroke are well defined.

During each stroke, all features change continuously. At each timestamp, we obtain the feature tuple $[\theta, \mathbf{\Delta h}, \mathbf{v}, \mathbf{x}, \mathbf{y}]$. RF-Copybook outputs the copybook which is a sequence of 4-dimensional feature tuples in time domain for each stroke:

$$[\theta, \mathbf{\Delta h}, \mathbf{v}, \mathbf{x}, \mathbf{y}] = \begin{bmatrix} \theta(t_s) & \Delta h(t_s) & v(t_s) & x(t_s), y(t_s) \\ \vdots & \vdots & \vdots & \vdots \\ \theta(t_{s+i}) & \Delta h(t_{s+i}) & v(t_{s+i}) & x(t_{s+i}), y(t_{s+i}) \\ \vdots & \vdots & \vdots & \vdots \\ \theta(t_e) & \Delta h(t_e) & v(t_e) & x(t_e), y(t_e) \end{bmatrix}. \tag{16}$$

The copybook for each stroke is a fine-grained quantification for the writing process. We implement RF-Copybook as a precise and intuitionistic calligraphy learning system through the following three steps.

- We first record the phase readings when the professional calligrapher is writing characters, segment the readings and process the data to establish each stroke's copybook.
- Then we measure the phase readings during the learner's writing process to extract each stroke's feature tuple.
- We then compare the feature tuple with the copybook for each segmented stroke within a character. The detail difference can be employed to guide the learner to correct his/her writing activity.

7 IMPLEMENTATION AND EVALUATION

In this section, we first introduce the implementation of RF-Copybook. Then we evaluate the performance of RF-Copybook and compare it with the state-of-the-art systems.

7.1 Implementation

Readers and tags: We use an Impinj Speedway R420 reader [7] and two cheap Alien tags [22] in our experiments. Three directional antennas, each with a 5 dBi gain are connected to the RFID reader. The reader is compatible with EPC Gen2 standard [5] and operates in the frequency range of 920.625 MHz to 924.375 MHz, which is the

[4]The distance between antenna 1 and antenna 3 is a.

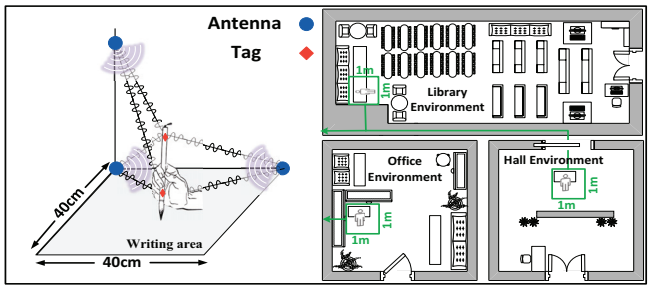

Fig. 20. The deployment layouts of three different environments.

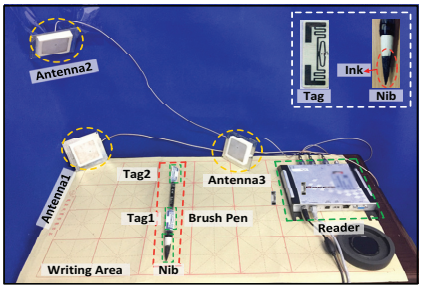

Fig. 21. The system setup in the office environment.

legal UHF band in China. During the data collection process, we let the reader hop over 8 channels where the adjacent channels are separated by 500 KHz. For each pair of antenna and tag, the reader collects phase and RSS measurements continuously. Hopping over 8 channels takes around 0.14 s to complete. In such a short time period, the location change of the tag is very small. Then the data collected at each location is prepared for estimating the antenna-tag distances.

Server and algorithm implementation: A laptop with 2.6 GHz CPU and 8 GB memory acts as the server to collect data and run our proposed method. The RFID reader communicates with the laptop with low level reader protocol (LLRP) [6]. The phase and RSS data collected by reader are forwarded to the laptop through an Ethernet cable. The proposed method is implemented in C# and Matlab.

Phase Calibration: To achieve a high distance estimation accuracy, we use the method introduced in §4 to remove the constant phase shift and reduce the amount of random noise.

Environment and system setup: We conduct experiments in three typical indoor environments with different levels of multipath: an empty hall, an office and a library corresponding to low, medium and high multipath environment. The deployment layout is shown in Fig. 20. In each environment, we place our prototype system on a desk to form a monitoring area, as shown in Fig. 21. Two tags are attached on the brush pen, and three antennas are connected to the reader. The antenna 1 is placed on at the coordinate origin, 2 is placed on the Z axis and 3 is placed on the Y axis. We use a common seen brush pen with a length of 29.8 cm in our experiments. The nib length is 5.5 cm. When the pen just touches the writing area perpendicularly, the pen's elevation distance is h=16 cm. The maximum nib length change is around 4 cm during the writing process. The distance between the two tags is b=16 cm. The distance between the antenna 1 and 2 equals to the distance between the antenna 1 and 3 with a = 40 cm. The writing area is a rice paper with a size of 40 cm × 40 cm. We move the brush pen at a speed around 1 − 2 cm/s and RF-Copybook is able to track 6 positions in one second.

7.2 End to end performance evaluation

7.2.1 Antenna-tag distance estimation accuracy. The antenna-tag distance estimation is evaluated in three different environments. In each environment, we write the 'horizontal' stroke with a length of 15 cm and repeat it 10 times. Fig. 22 shows the average antenna-tag distance accuracies. The average distance errors in the three environments are 4.8 mm, 6.5 mm and 7.5 mm, respectively. The distance estimation method provides a millimeter accuracy even in the high multipath library environment. On the other hand, if we estimate the distance without our clean phase selection method, the accuracies decrease to 6.7 mm, 18.4 mm and 20.3 mm, respectively.

We also test the system performances in different monitoring sizes and vary the distance between the antenna and tag from 20 cm to 100 cm. As shown in Fig. 23, when the distance between the antenna and tag is larger than 60 cm, the accuracies of distance estimation are decreased. The main reason is when the distance becomes larger,

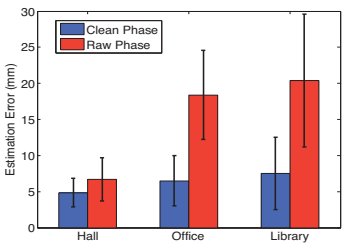

Fig. 22. Antenna-tag distance accuracy.

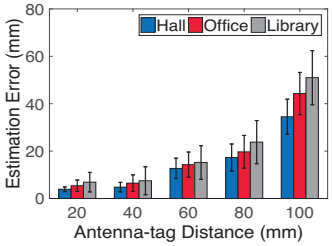

Fig. 23. Different antenna-tag distances.

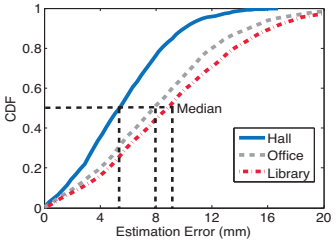

Fig. 24. Elevation distance accuracy.

the phase rotation is larger than 2π and get wrapped to a value between 0 and 2π. And thus we need to obtain the accurate phase rotation number k with the help of RSS readings. However, RSS readings are relatively coarse compared to phase readings and thus the distance estimation error becomes large. For the learners, the area of writing is relatively small. To provide a reliable tracking performance, currently we set the monitoring region to 40 cm×40 cm.

7.2.2 Elevation distance accuracy. Based on the antenna-tag distances, the elevation distance of the brush pen can be estimated according to (9). To evaluate the elevation distance, we repeat lifting the brush pen from the writing surface with a height of 5 cm for 50 times. Fig. 24 shows the cumulative distribution function (CDF) of distance estimation errors in three different environments. From the figure, we can see that median errors are 5.9 mm, 7.8 mm and 9.4 mm, respectively. The nib's length change is closely related to the elevation distance change. So the nib's length change accuracy is similar to the elevation distance accuracy and we neglect the repeated evaluations.

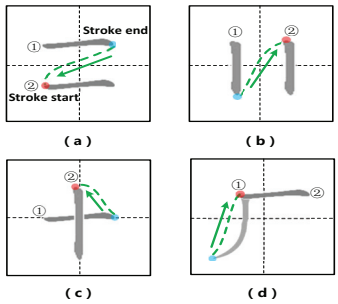

Fig. 25. Four types of stroke transition.

7.2.3 Stroke segmentation accuracy. Based on the elevation distance change, the phase readings can be segmented into strokes. To obtain the stroke segmentation ground truth, we use a camera to record the process. If the difference between the identified timestamps and the ground truth is within 1 second, we consider RF-Copybook correctly identifies the segmentation time point. The stroke segmentation accuracy are evaluated through the following three experiments:

(i) We consider four types of stroke transitions as illustrated in Fig. 25. Each stroke length is about 15 cm. We repeat each transition type for 50 times. The results are presented in Fig. 26. The segmentation accuracies are always higher than 90%.

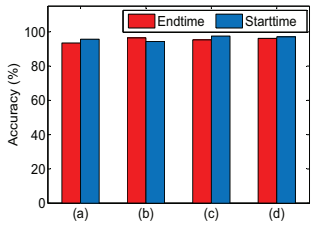

Fig. 26. Stroke segmentation with different types of stroke transition.

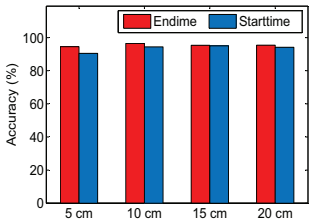

Fig. 27. Stroke segmentation with different stroke length.

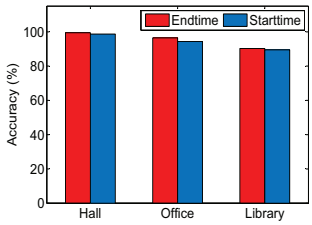

Fig. 28. Stroke segmentation in different environments.

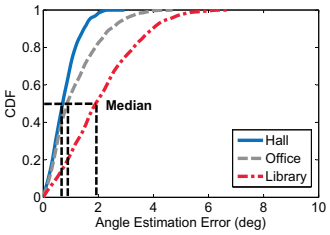

Fig. 29. Elevation angle accuracy.

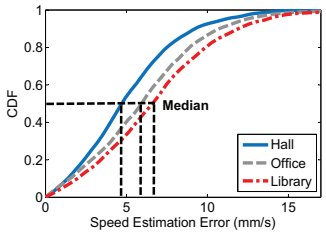

Fig. 30. Nib's speed accuracy.

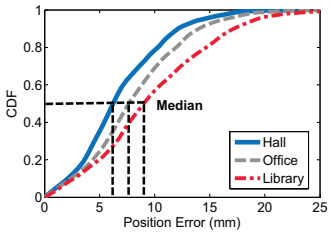

Fig. 31. Nib's position accuracy.

(ii) When the stroke length changes, the transition distances between the same two strokes are different. We use the stroke transition type (b) as the default setup. Four different stroke lengths are compared in Fig. 27. Each stroke length is repeated 50 times. We can see that the stroke length does not affect the segmentation accuracy.

(iii) We also evaluate the segmentation accuracy in different environments. The default stroke transition type is repeated 50 times in three different environments. The results are presented in Fig. 28. RF-Copybook achieves consistent high segmentation accuracies across different environments. However, we do observe slightly lower accuracies in the library environment due to more multipath.

7.2.4 Elevation angle accuracy. To evaluate the angle estimation accuracy proposed in RF-Copybook, we place the pen on the writing area, then we change the angle between the pen and the writing surface from 0° to 90° with a step of 3°. For a specific angle setup, we get the ground truth by measuring the angle value with a protractor. The experimental results are shown in Fig. 29. Even in the library environment with rich multipath, RF-Copybook achieves a median angle estimation accuracy of 2° which is accurate enough for our application.

7.2.5 Nib's moving speed accuracy. We write a 'horizontal' stroke for 10 times and evaluate the nib's speed measurement accuracy. We record the ground truth with the help of a stopwatch and a range meter. Fig. 30 shows the estimation results in different environments. We can see that the median errors are 4.6 mm/s, 5.6 mm/s and 6.8 mm/s, respectively. These high accuracies benefit from very accurate antenna-tag distance estimates.

7.2.6 Nib's position accuracy. The nib's position is a key indicator for the stroke's relative position inside the whole character. We choose 50 locations during the writing process in each environment for this evaluation. The experimental results of the Euclidean distances between the ground truth and the estimated results are shown in Fig. 31. The median errors in three environments are 6.5 mm, 7.8 mm and 8.8 mm, respectively. RF-Copybook can be easily applied to provide high accuracy localization in other tracking applications.

7.2.7 User perception. First, we introduce how our system guide the learner to improve the writing process. Specifically, we ask an expert and a learner to write a same Chinese character 'Big'. Then we apply our system to monitor the writing processes and extract the feature tuple $[\theta, \mathbf{\Delta h}, \mathbf{v}, \mathbf{x}, \mathbf{y}]$. By comparing the feature tuples of the expert and learner, we can obtain the places where the learner did not perform well.

The written trajectories are shown in Fig. 32. When compared with the expert's trajectory, the learner's trajectory is coarse and inaesthetic. Firstly, the relative positions of different strokes are not correct for the learner's writing. This can been improved by correcting the nib's position $[\mathbf{x}, \mathbf{y}]$ for each stroke based on the difference between the learner and the expert. Secondly, the strokes are uneven and stiff due to the non-smoothing writing speed. The learner can be guided by the difference of nib's moving speed $\mathbf{v}$ with respect to the expert's writing. At last, the stroke widths are different and we take the 'Horizontal' stroke as an example. For the stroke written by the expert, the width is moderate and becoming thicker from left to the right side along the stroke. While the stroke width written by the learner varies randomly. We can thus compare the elevation angle θ and nib's length change $\mathbf{\Delta h}$ between the two writings. The differences tell the learner to reduce the brush pen's inclination and the pressure exerted on the writing surface. Consequently, the stroke width problem can be mitigated.

Then to test the user perception of our system, we ask twenty volunteers to write the same characters and monitor their writing processes. Each volunteer repeats the writing 10 times. We extract the feature tuples from the readings and set the expert's feature tuple as the copybook. Then we compare the volunteers' feature tuple with the copybook and use the difference to guide the volunteer's writing. Seventeen of them consider our system are helpful in improving their writing. Therefore, based on the tracking information, the system provides detailed suggestions to the leaner to improve the writing at each place not performed well.

7.3 Comparison with the-state-of-art systems

We compare RF-Copybook against *Tagoram* [32], *RF-IDraw* [26] and *PolarDraw* [17] on the performance Chinese character recognition accuracy. To compare with these systems fairly, the other systems are set to their optimal performance conditions.

For Tagoram, we deploy 4 antennas along Y axis which is at the upper side of the monitoring region. The spacing between adjacent antennas is 10 cm. Because Tagoram requires a large amount of data to build hologram for location estimation, we collect about 50 readings from each antenna. In addition, we set the writing speed as low as possible (approximately 0.3 cm/s) to ensure that Tagoram is able to collect enough amount of data at each location. For RF-IDraw, we deploy 4 antennas with two antennas have a spacing of half wavelength (16 cm) between them along the Y axis. Another two antennas have a spacing of 1.5× wavelength (48 cm) along the X axis at the left side of the monitoring region. To combat against noise, each antenna collects 5 readings for processing. For PloarDraw, we place two linearly polarization antennas at the upper side. Antenna 1 is placed at the coordinate origin and antenna 2 is placed along the Y axis with a distance of 40 cm to the coordinate origin.

7.3.1 Chinese character recognition accuracy. We divide the tested Chinese characters into five groups based on the number of strokes in each character. For each group, we randomly choose 10 characters and evaluate the recognition accuracy for the four systems. Fig. 34 shows the results on the recognition accuracies. When there is only one stroke, all the four systems achieve high recognition accuracies over 92%. When the number of strokes increases, the recognition accuracies of *Tagoram*, *RF-IDraw* and *PolarDraw* decrease sharply; while the accuracy of RF-Copybook is still higher than 95%. The high accuracy is mainly from its stroke segmentation ability, i.e., RF-Copybook can recognize each stroke of a Chinese character separately which improves the overall recognition accuracy. However, the other three systems can not separate the strokes accurately, resulting in relatively large recognition errors.

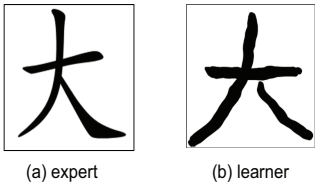

Fig. 32. Trajectories under different levels of expertise.

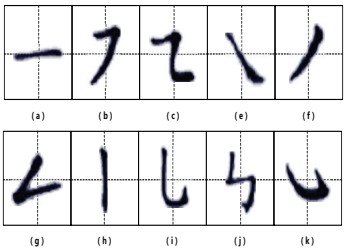

Fig. 33. 10 kinds of tested strokes.

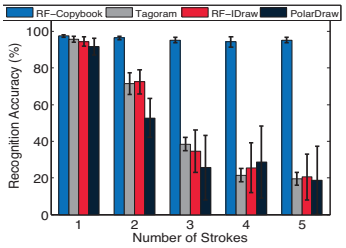

Fig. 34. Chinese character recognition accuracy.

7.4 Discussion

We discuss some limitations and opportunities for system improvement.

Limitation on brush pen's moving speed. The performance of RF-Copybook may decrease when the pen moves at a high speed, e.g., above 30 mm/s. In this scenario, the movement of tags attached on the pen introduces non-negligible additional phase change due to the Doppler effect, which results in distance estimation errors and performance degradation. In our future work, we will address the Doppler effect to make RF-Copybook robust against high moving speeds.

Limitation on the size of the monitoring area. The monitoring area required for calligraphy writing is relative small. In a small area with relative short distance between tag and antenna, it is easy to achieve mm-level distance estimation accuracy due to very little multipath and high Signal to Noise Ratio (SNR). However, it is hard to achieve millimeter level accuracy when the antenna-tag distance is much larger in a room size level. For example, *PinIt* [26] achieves a best accuracy of 11 cm in a typical indoor environment with the antenna-tag distance between 3 to 7 meters. To achieve a mm-level accuracy in a larger area, one possible solution is to deploy more antennas which is a trade-off between infrastructure cost and accuracy.

8 RELATED WORK

In this section, we compare RF-Copybook to existing works from multiple areas, including the image based calligraphy models, RFID based high accuracy tracking systems, other localization and activity recognition approaches.

Image based calligraphy models. There are many image based calligraphy models proposed recent years to assist the calligraphy learners. Work [31] sets good writing examples by extracting the stroke's width and strokes order from the screen shots of the writing process. To extract the stroke's feature, a geometric approach is proposed in [21] for the robot to compose a character. Similarly, robot is augmented with the ability to perceive and cognize the brush footprint profile based on the proposed model in [10]. By learning the calligrapher's written works, [11] can synthesize the Chinese calligraphy with a similar topological style. [33] can animate the writing process by determining the quantitative values of parameters based on the character shape. [35] constructs a retrieval engine thus the dynamic writing process are simulated for learners to watch. In [27], a hierarchical evaluation approach which involves the evaluations for the whole character and each stroke is proposed, it calculates the stroke shape similarities between the leaner's calligraphy and the standard calligraphy. However, these approaches are unable to tell the learner the difference of brush pen's movement feature from the calligrapher, it is still hard for the learner to improve the calligraphy skills. In contrast, RF-Copybook can quantify the writing process from the aspect of the pen's movement. The four features proposed reflect the stroke width and character structure well, thus can provide a helpful guidance for the learners.

RFID based high accuracy tracking systems. *RF-IDraw* [26] is the first RFID based system that can accurately track a user's writing or gesturing in the air. It requires eight antennas to locate rigidly and form an array. The distance between the antenna and the tag is required to be much larger than the spacing between antennas. When the monitoring area is small and the distance between tag and reader is large, the movement-caused direction change is subtle and thus it is challenging for RF-IDraw to detect such small-scale movement. *Tagoram* [32] uses four reader antennas to real-time track a moving tag and achieves an accuracy of centimeter level. Tagoram employs the similarity between measured phases and theoretical values to estimate the movement trajectory, achieving a high accuracy. However, for calligraphy writing, the trajectory is unknown priori. In this scenario, Tagoram's accuracy is much lower, not high enough for calligraphy monitoring even in a small scale. To translate the pen's moving on the whiteboard, *PolarDraw* [17] deploys two antennas and uses RSS readings to estimate tag's moving direction when the receiving antenna's polarization angle mismatches the tag's antenna, then combines the moving distance estimated by the phase differences to track the trajectory. The trajectory accuracy is about 10 cm, which is much lower than the requirement calligraphy monitoring. Although those systems can track the tag's trajectory, they cannot estimate the tag's absolute location information. In fact, the absolute location is a key factor to reflect the stroke's structures related to the whole character. *STPP* [18] is another tag order sortation system with an accuracy of centimeter level. However, it cannot localize the tag's position and thus is not applicable for motion tracking. *PinIt* [25] is another work built on RFID to localize tags based on the multipath profile similarity with the reference tags. The localization accuracy is about 12 cm. In addition, a large number of reference tags are required and a moving antenna is needed to formulate the antenna-array. Those works are all RFID based and with a relatively high accuracy. However they are unsuitable in the application of brush pen's trajectory trace for Chinese calligraphy learning, because a 6 cm over accuracies are far from enough for characterizing the moving features. Instead, RF-Copybook utilizes the millimeter accuracy antenna-tag distance to realize the 3-dimensional localization and tracking.

Other tracking methods. There are many other fine-grained tracking systems. [3] utilizes the change pattern of gyroscope and accelerometer to tracks the smartphone's motion in the air. [23] uses that sensors on the smartwatch to infer the tying word on the keyboard. By wearing the smartwatch and utilizing the sound signal, [12] achieves a high accuracy of 8 mm. However, the accuracy degrades a lot when there are interference around the hand. [34] uses the acoustic signal to estimate the doppler shift and track the smartphone. When there are interference and severe multipath effects in the environment, the accuracy decreases dramatically. Moreover, some device free and passive tracking systems are proposed. *WiDraw* [20] uses 30 neighboring Wi-Fi devices to track a 25 cm writing width with an accuracy about 5 cm. *WiTrack* [2] and *WiTrack 2.0* [1] rely on the specialized software-defined radio to achieve centimeter level localization accuracy. *mTrack* [29] uses the millimeter-wave to track a pen and achieve a high accuracy to 8 mm. However, the system costs too expensive to be practically used. Compared to those systems, RF-Copybook provides a millimeter level localization accuracy and robust to the multipath and environment noise.

Localization and activity recognition approaches. Some fine-grained physical layer channel information based localization approaches are proposed recent years. Those works either use the model based or training based methods to localize a smartphone with the best accuracy of submeter [8, 9, 15, 16]. However, the submeter accuracy is insufficient for fine-grained tracking a brush pen. *LiFS* [24] models the wireless propagation channels mathematically and estimates the target location from the distorted CSI measurements. It achieves a meter-level localization accuracy but still can not be applied to millimeter level accuracy application. Many systems human activity or gesture recognition approaches have been proposed [4, 13, 14, 28]. Some systems, like *E-Gesture* [14] and *RisQ* [13], employ the gyroscope and accelerometer readings to characterize different kinds of predefined hand gestures. Those systems, however, can not provide the exact location of a human part (e.g., hand) and the recognition errors increase over time. Thus, those systems can not be applied to solve the problem addressed in this paper. Other systems use the RF signal and can provide reliable accuracy over time. Specifically, *E-eyes* [28]

classifies different activities based on the CSI measurements caused by human motion. *WiKey* [4] recognizes user input on keyboards by analyzing the CSI pattern of the Wi-Fi signals distorted by human fingers. However, these systems need lots of training effort and only can identify predefined coarse-grained activities, and hence cannot be directly applied to the fine-grained writing recognition since writing style varies from person to person. Different from those labor-intensive or error unbearable approaches for writing process tracking, RF-Copybook achieves a millimeter accuracy benefits from the fine-grained phase values.

9 CONCLUSION

To monitor and quantify the writing process of Chinese calligraphy, we propose a RFID based system RF-Copybook. By attaching two passive tags on the brush pen and use three antennas at the RFID reader, we build a cost efficient and easy-to-implement system. RF-Copybook relies on the phase readings from multiple frequency channels to extract clean direct path phase information for accurate distance estimation. With multiple antenna-tag distances, RF-Copybook segments the phase readings into strokes and then models each stroke's features along the writing process. Extensive experiments validate that RF-Copybook is effective and robust in characterizing the writing process. Thus, by comparing the feature differences with the professional calligrapher's writing, the learner knows how to change their writing process to improve the writing skill intuitively.

10 APPENDIX

Claim: when the carrier frequency changes, the rotation number k remains unchanged.
To validate this claim, we suppose two different carrier frequencies f_m and f_n. A typical ImpinJ Speedway R420 reader works at 16 channels with carrier frequencies from 920.625 MHz to 924.375 MHz [7]. Thus the phase difference is:

$$2d \times 2\pi \times \frac{f_m - f_n}{c} < \frac{d}{40} \times 2\pi, \tag{17}$$

That is to say, if the distance d is smaller than 40 m, the phase difference between different channels is smaller than 2π and the rotation number k remains unchanged. In practice, the reader's operating range is about 10 m [7]. Therefore, the phase rotation numbers at different channels are the same.

REFERENCES

[1] Fadel Adib, Zachary Kabelac, and Dina Katabi. 2015. Multi-person localization via RF body reflections. In *USENIX NSDI*. 279–292.
[2] Fadel Adib, Zachary Kabelac, Dina Katabi, and Robert C Miller. 2014. 3D tracking via body radio reflections. In *USENIX NSDI*. 317–329.
[3] Sandip Agrawal, Ionut Constandache, Shravan Gaonkar, Romit Roy Choudhury, Kevin Caves, and Frank Deruyter. 2011. Using mobile phones to write in air. In *ACM Mobisys*. 15–28.
[4] Kamran Ali, Alex X Liu, Wei Wang, and Muhammad Shahzad. 2015. Keystroke recognition using WiFi signals. In *ACM MobiCom*. 90–102.
[5] EPCglobal EPC Gen2. 2017. www.gs1.org/epcglobal. (2017).
[6] Aug EPCglobal Inc. 2007. Low Level Reader Protocol, Version 1.0. 1. (2007).
[7] Inc Impinj. 2017. www.impinj.com/products/readers/speedway-revolution/. (2017).
[8] Manikanta Kotaru, Kiran Joshi, Dinesh Bharadia, and Sachin Katti. 2015. SpotFi: decimeter level localization using WiFi. *Acm Sigcomm Computer Communication Review* 45, 4 (2015), 269–282.
[9] Swarun Kumar, Stephanie Gil, Dina Katabi, and Daniela Rus. 2014. Accurate indoor localization with zero start-up cost. In *ACM MobiCom*. 483–494.
[10] Josh HM Lam and Yeung Yam. 2011. Application of brush footprint geometric model for realization of robotic Chinese calligraphy. In *International Conference on Cognitive Infocommunications*. 1–5.
[11] Wei Li, Yuping Song, and Changle Zhou. 2014. Computationally evaluating and synthesizing Chinese calligraphy. *Neurocomputing* 135 (2014), 299–305.
[12] Rajalakshmi Nandakumar, Vikram Iyer, Desney Tan, and Shyamnath Gollakota. 2016. FingerIO: using active sonar for fine-grained finger tracking. In *ACM CHI*. 1515–1525.

[13] Abhinav Parate, Meng-Chieh Chiu, Chaniel Chadowitz, Deepak Ganesan, and Evangelos Kalogerakis. 2014. RisQ: Recognizing Smoking Gestures with Inertial Sensors on a Wristband. In *ACM Mobisys*. 149–161.
[14] Taiwoo Park, Jinwon Lee, Inseok Hwang, Chungkuk Yoo, Lama Nachman, and Junehwa Song. 2011. E-gesture: a collaborative architecture for energy-efficient gesture recognition with hand-worn sensor and mobile devices. In *ACM SenSys*. 260–273.
[15] Souvik Sen, Romit Roy Choudhury, Bozidar Radunovic, and Tom Minka. 2011. Precise indoor localization using PHY layer information. In *ACM Mobisys*. 413–414.
[16] Souvik Sen, Bo Radunovic, Romit Roy Choudhury, and Tom Minka. 2012. You are facing the Mona Lisa: spot localization using PHY layer information. In *ACM Mobisys*. 183–196.
[17] Longfei Shangguan and Kyle Jamieson. 2016. Leveraging electromagnetic polarization in a two-antenna whiteboard in the air. In *ACM CoNEXT*. 443–456.
[18] Longfei Shangguan, Zheng Yang, Alex X Liu, Zimu Zhou, and Yunhao Liu. 2015. Relative localization of RFID tags using spatial-temporal phase profiling. In *USENIX NSDI*.
[19] Cao Shi, Jianguo Xiao, Wenhua Jia, and Canhui Xu. 2013. Character feature integration of Chinese calligraphy and font. In *DRR*. 86580M.
[20] Li Sun, Souvik Sen, Dimitrios Koutsonikolas, and Kyu Han Kim. 2015. WiDraw: enabling hands-free drawing in the air on commodity WiFi devices. In *ACM MobiCom*. 77–89.
[21] Yuandong Sun, Huihuan Qian, and Yangsheng Xu. 2014. A geometric approach to stroke extraction for the Chinese calligraphy robot. In *IEEE International Conference on Robotics and Automation*. 3207–3212.
[22] Alien Tags. 2017. www.alientechnology.com/tags/. (2017).
[23] He Wang, Tsung Te Lai, and Romit Roy Choudhury. 2015. MoLe: Motion Leaks through Smartwatch Sensors. In *ACM MobiCom*. 155–166.
[24] Ju Wang, Hongbo Jiang, Jie Xiong, Kyle Jamieson, Xiaojiang Chen, Dingyi Fang, and Binbin Xie. 2016. LiFS: low human-effort, device-free localization with fine-grained subcarrier information. In *ACM MobiCom*. 243–256.
[25] Jue Wang and Dina Katabi. 2013. Dude, where's my card? RFID positioning that works with multipath and non-line of sight. *ACM Sigcomm Computer Communication Review* 43, 4 (2013), 51–62.
[26] Jue Wang, Deepak Vasisht, and Dina Katabi. 2014. RF-IDraw: virtual touch screen in the air using RF signals. *ACM Sigcomm Computer Communication Review* 44, 4 (2014), 235–246.
[27] Mengdi Wang, Qian Fu, Zhongke Wu, Xingce Wang, and Xia Zheng. 2014. A hierarchical evaluation approach of learning Chinese calligraphy. *Journal of Computational Information Systems* 10, 18 (2014), 8093–8107.
[28] Yan Wang, Jian Liu, Yingying Chen, Marco Gruteser, Jie Yang, and Hongbo Liu. 2014. E-eyes: device-free location-oriented activity identification using fine-grained WiFi signatures. In *ACM MobiCom*. 617–628.
[29] Teng Wei and Xinyu Zhang. 2015. mTrack: high-precision passive tracking using millimeter wave radios. In *ACM MobiCom*. 117–129.
[30] Sam Tak-sum Wong, Howard Leung, and Horace Ho-shing Ip. 2006. Fitting ellipses to a region with application in calligraphic stroke reconstruction. In *IEEE Image Processing*. 397–400.
[31] Yingfei Wu, Yueting Zhuang, Yunhe Pan, and Jiangqin Wu. 2006. Web based chinese calligraphy learning with 3D visualization method. In *IEEE Multimedia and Expo*. 2073–2076.
[32] Lei Yang, Yekui Chen, Xiang Yang Li, Chaowei Xiao, Mo Li, and Yunhao Liu. 2014. Tagoram: real-time tracking of mobile RFID tags to high precision using COTS devices. In *ACM MobiCom*. 237–248.
[33] Lijie Yang and Xiaoshan Li. 2009. Animating the brush-writing process of Chinese calligraphy characters. In *IEEE/ACIS Conference on Computer and Information Science*. 683–688.
[34] Sangki Yun, Yi Chao Chen, and Lili Qiu. 2015. Turning a mobile device into a mouse in the air. In *ACM Mobisys*. 15–29.
[35] Yueting Zhuang, Xiafen Zhang, Weiming Lu, and Fei Wu. 2005. Web-Based Chinese Calligraphy Retrieval and Learning System. In *ICWL*. 186–196.

Received May 2017; revised August 2017; accepted October 2017